Influence of surface treatments and addition of a reactive agent on the properties of PLA/flax and PLA/bamboo composites

Hervé Nlandu-Mayamba, A. Taguet, Perrin Didier, Sébastien Joannès, Florence Delor-Jestin, Haroutioun Askanian, J. Lopez-Cuesta

Influence of surface treatments and addition of a reactive agent on the properties of PLA/flax and PLA/bamboo composites

Hervé Nlandu-Mayamba[1], Aurélie Taguet[1], Didier Perrin[1], Sébastien Joannès[2], Florence Delor-Jestin[3], Haroutioun Askanian[3] and José-Marie Lopez-Cuesta[1]

[1]Polymers Composites and Hybrids (PCH), IMT Mines Ales, Ales, France
[2]MINES Paris, CNRS UMR, PSL University Centre des Matériaux (MAT), Evry Cedex, France
[3]Clermont Auvergne Université, UMR CNRS 6296, CA INP, ICCF Institut de Chimie de Clermont-Ferrand, Aubière, France

Corresponding author:
José-Marie Lopez-Cuesta, Polymers Composites and Hybrids (PCH), IMT Mines Ales, 6 Avenue de Clavières, Alès 30319, France.
Email: jose-marie.lopez-cuesta@mines-ales.fr

Abstract

Polylactic acid (PLA) composites reinforced with 10 wt% of flax (FF) or bamboo (BF) fibers were prepared via an internal mixer and/or twin-screw extrusion. Alkali pretreated fibers were soaked in silane to improve adhesion between fibers and matrix. 0.8 wt% of Joncryl™, a grafted copolymer acting as PLA chain extender, was also used alone or in combination with silane treatment of fibers to improve interfacial adhesion. The influence of silane treatment and/or Joncryl on the composite materials on mechanical, thermal and thermomechanical properties of materials processed through injection molding was investigated. Improved adhesion of the fibers to the matrix was shown using a scanning electron microscope. Fourier Transform Infrared Spectroscopy indicated that chemical bonds were formed between the silane coupling agent and fibers. X-ray Photo-electron Spectroscopy confirmed that fibers and silane derivatives were effectively coupled. XPS also highlighted that silane coupling agent reacted in higher amounts on bamboo than flax fibers, probably due to a higher amount of lignin in the case of bamboo fibers. Ther-mogravimetric analyses indicated that silane-treated flax and bamboo increased the thermal stability of the corresponding composites (PLA-SFF and PLA-SFB) compared to non-treated fiber composites. The incorporation of Joncryl alone entailed a degradation of the thermal stability of the corresponding composites (PLAJ-FF and PLAJ-FB) but

enhanced the PLA/fibers interfacial adhesion. The combination of Joncryl and silane treatment resulted in strong improvements of thermal stability and interfacial adhesion for the PLAJ-SFF and PLAJ-SBF composites. Increase in tensile moduli and decrease in tensile strengths with the incorporation of the pristine fibers were noted. For silane-treated fibers, the tensile modulus and the strength of the corresponding composites were improved when adding Joncryl alone or in combination with silane. From also rheological and molar weight measurements, it could be concluded that Joncryl acts both as PLA chain extender and coupling agent.

Keywords
Fibers, surface treatment, joncryl, interfacial adhesion, biocomposite

Introduction

The development of biodegradable and renewable polymeric materials as natural fiber composites is increasing significantly regarding their economic and ecological advantages.[1,2]

In this context, PLA, which belongs to the family of aliphatic polyesters, is one of the main representatives of the biodegradable polymers. It has high transparency, modulus, strength, good barrier properties and competitive price, comparable to many petroleum-based plastics.[3] Nevertheless, some drawbacks of PLA, such as poor toughness, high brittleness, low glass transition and heat distortion temperature, limit its usage in many applications.[4] In connection with this, the natural fibers extracted from plants have been used as a reinforcement in polymer matrices, which is a handy way to improve the overall PLA polymer properties.[5] A significant issue related to biocomposites is the poor adhesion of the fibers to the matrix, due to the strongly polarized hydroxyl groups of lignocellulose. The challenges and concerns posed by the PLA and incompatibility between the PLA and fiber have been and are being addressed by many researchers. These limitations could be alleviated through chemical modifications, reinforcement, plasticizing, addition of coupling agents, and others.[6]

It is well known that surface treatments of lignocellulosic materials create some structural modifications influencing interfacial bonding with the matrix. Alkali and silane treatments are the most commonly used and often adopted chemical treatment to decrease the fibers hydrophilic nature, thus improving their compatibility with most matrices.[7]

In the specific case of sisal fibres reinforced composite, the interfacial adhesion between PLA and fibres has been improved via in situ reactive compatibilization at molten state with the addition of an epoxy oligomer.[8] Joncryl ADR, a kind of commercial grade multifunctional styrene acrylic oligomer, which we consider having potential for effective reactive compatibilization in natural fiber reinforced polymer composites, has epoxy functions showing effective reactivity with hydroxyl groups and carboxylic acids of the PLA chains. This allows it to act as a chain extender [9–11] and would also react with the hydroxyl groups of the fibers, thus acting as a coupling agent or possibly react with the chain end of a silane grafted at the surface of the fiber.

In this work, the effect of (3-aminopropyl) triethoxysilane (APS) and/or chain extender Joncryl ADR content on PLA/flax or bamboo fiber mat composites, was assessed.

Joncryl, which acts mainly as a chain extender, is used in this article to promote interfacial adhesion between the two natural fibers (flax and bamboo) modified with silane and the PLA matrix. This was evaluated by regarding the mechanical, thermal and thermomechanical properties of the composites.

Materials and methods

Materials

PLA used in this study was a transparent film-grade PLA 4043D from NatureWorks LLC (Minnetonka, MN, USA), available in pellet form, with the density of 1.24 g/cm^3 containing 4.8% D-lactide. The glass transition temperature (Tg) of this biopolymer is about 55°C–60°C and the melting point (Tm) is in the range 145°C–160°C. Nevertheless, the crystallization rate of PLA 4043D is very low and the material is nearly amorphous [12] The melt flow index (MFI) of the tested polylactide is 6 g/10 min at 190°C under the load of 2.16 kg (according to the D1238 ASTM standard).

Lignocellulosic biomasses used in this work are flax tow and bamboo shavings. Flax tow is a non-woven fiber by-product resulting from the scutching of flax. A length of 6 mm (fiber diameter of around 10 μm) was cut and supplied by Terre de lin (St Pierre le Viger, France). While bamboo shavings of around 300 μm in length (fiber diameter of around 100 μm) are wastes from the manufacture of continuous ribbons of single unidirectional bamboo fiber obtained by a high-tech process developed and patented by Cobratex (Carbonne, France). The respective fractions of cellulose, hemicellulose and lignin are respectively 80, 13, two for flax, and 55, 11, 22 for bamboo fibers, according to Dorez et al.[13]

Joncryl ADR 4468 from BASF's company is a copolymer consisting of a styrenic unit, an acrylic acid unit and a glycidyl methacrylate unit and was used as a reactive compatibilizer. It has epoxy functions, whose reactivity with polycondensates (polyesters, polycarbonates, polyamides) allows it to play the role of chain extender and potential interfacial coupling agent.

Fibers surface treatment

Fibers were first pretreated by mercerization. They were soaked in a solution of 5 wt% sodium hydroxide (NaOH) at room temperature for 3 h. Then, the fibers were washed several times with water until neutral pH was obtained, to remove residual alkali and oven-dried at 60°C for 24 h.

Secondly, the pretreated fibers with NaOH were treated by silylation. The pretreated fibers were immersed for 1 h in a 1 wt% solution of (3-aminopropyl) triethoxysilane (APS) prepared in acetone, adjusted to pH 3.5 with acetic acid. Then, fibers were filtered, oven-dried at 65°C for 12 h, then carefully washed with water and oven-dried again at 80°C overnight.

Compounding

A masterbatch of PLA/flax (70/30 wt%) and 0.8 wt% Joncryl was made in a rotating internal laboratory mixer (Haake Rheomix 3000) equipment operated with roller rotors at 185°C and 50 r/min. The obtained pre-compound saturated with flax fibers (30 wt%) was cut out in small particles and ground in Alpine cutting mill using a sieve of 8 mm in diameter in order to recover the ground pre-compound. The masterbatch was then ground and diluted in the PLA matrix in order to have a final composite containing 10 wt% flax fibers and maintaining 0.8% Joncryl.

To dilute the masterbatch, the extrusion was carried out by a BC21 Clextral co-rotating twin-screw extruder (21 mm screw diameter and a 900 mm screw length) with two feeders. Prior to extrusion, the polymer granules and fibers were vacuum dried overnight at 65°C. 12 modules constitute the heating barrel system, set from 60°C at the inlet of module 1 to 185°C on the rest of barrel. The screw speed was set at 250 r/min, with a total feed rate of 5 kg/h.

For bamboo-based composites, PLA pellets were introduced through the first feeding hopper located at the entrance of module one of the barrel and the 10 wt% bamboo fiber incorporation was made through the second one located on module 5, also, Joncryl was gradually introduced in a quantity corresponding to the total flow rate of the system for a total of 0.8 wt%, through the second one located on module 5. Whereas for flax-based composites, the shredded and diluted pre-compound in the virgin PLA matrix were all introduced through the first feeding hopper and a total of 0.8 wt% Joncryl was also gradually introduced into the second hopper on the module 5 as described above.

To the output of the extruder, filament-shaped compounds were cooled in a water bath and quickly dried by air pulses, and finally granulated. The pellets thus obtained were dried under vacuum overnight at 65°C in order to remove residual moisture.

PLAJ-FF and PLAJ-BF are composites containing Joncryl (0.8 wt%) and flax and bamboo fibers (10 wt%), respectively.

Injection molding

A Krauss-Maffei KM50-T180CX press was used to manufacture dogbone samples ISO 1A according to ISO 527-2. The temperature profile was 195°C-195°C-195°C-195°C and 210°C for the nozzle. The injection pressure was 600 bars during 15 s for first stage, then 500 bars during 15 s for the second one, and the mould temperature was fixed at 30°C. The plasticization and injection speeds were set respectively at 100 r/min and 20 $cm^3\ s^{-1}$, while the cooling time was 15 s.

Characterizations

Fourier transform infra-red spectrometry. FTIR was carried out to assess the change of specific chemical groups of fibers before and after silane treatment. A Vertex 70 FTIR spectrometer (Bruker, Billerica (MA, USA) was used in ATR mode (Attenuated Total Reflectance) to measure spectra from 400 to 4000 cm^{-1} with a 4 cm^{-1} resolution and an

average of 32 scans recorded for each spectrum. The mentioned bands were normalized with the 1018 cm^{-1} band attributed to the C-O/C-C stretching vibrations. This band was chosen as a reference due to its sparsely change during silane treatment.

X-ray photoelectron spectroscopy. An ESCALAB 250 photoelectron X-ray spectrometer (Thermo Electron, Waltham (MA), USA) was used, with an Al Kα line (1486.6 eV) monochromatic excitation source. Samples analyzed were dried natural fibers. The analyzed surface had a diameter of 500 µm. Spectra were recorded from at least three different locations on each sample, with a 1 × 1 mm^2 area of analysis. The depth of the XPS probe was about 10 nm. The photoelectron spectra were calibrated in binding energy with respect to the energy of the C-C compounds of carbon C1s at 284.8 eV. The charge was compensated by a low energy electron beam (−2 eV).

Scanning electron microscope. Composites were cut using liquid nitrogen leading to cryo-fractured PLA composites. Composite fracture surface morphology was studied using a Sigma 300 scanning electron microscope (Carl Zeiss Microscopy, Oberkochen, Germany). All specimens were sputter coated with gold/palladium (Au/Pd) prior to examination to provide enhanced conductivity

Thermogravimetric analysis. The thermal stability of the materials was conducted on a TGA 4000 thermogravimetric instrument (Perkin Elmer, Waltham (MA), USA) under an inert gas (nitrogen) from 25 to 700°C at a heating rate of 10°C min^{-1}.

Differential scanning calorimetry. DSC thermograms of the biocomposites were performed using a DSC 3 (Mettler Toledo, Greifensee, Switzerland). An average weight of about 10 mg was sealed in aluminum pans, held for 2 min at 0°C, submitted to a first heating up to 200°C, held at 200°C for 1 min, followed by a cooling cycle to 0°C and maintained for 1 min at 0°C. Finally, a second heating up to 200°C was conducted. All the stages were conducted under a nitrogen atmosphere using a heating rate of 10°C/min with a flow of 20 mL/min.

Glass transition temperature (Tg), cold crystallization temperature and corresponding enthalpy (Tc and ΔHc) as well as melting temperature and corresponding enthalpy (Tm and ΔHm) were determined from the second heating cycle using the STARe system software. The crystalline index (X_C) was calculated according to equation (1):

$$X_C(\%) = \frac{\Delta H_m - \Delta H_c}{W \times \Delta H_0} * 100 \quad (1)$$

Where, ΔHm is the melting enthalpy of the sample, ΔH_0 is the melting enthalpy of 100% crystalline PLA, taken as 93 J/g.[5] ΔH_c is the crystallization enthalpy and W is the weight fraction of PLA in the biocomposite.

Rheology. The viscoelastic behavior of the materials accounting for modifications of possible phenomena of chain scission or cross-linking was investigated by following the

evolution of the complex viscosity as a function of time. A stress/strain-controlled MCR 302 rheometer (Anton Paar, Graz, Austria) was used to perform tests in oscillatory shear mode, with parallel plate equipment at a fixed temperature of 185°C. The diameter of the plates was 25 mm, and the gap between them of 1.7 mm, with an angular frequency of 6.28 rad.s^{-1} and a shear strain of 0.01% for 40 min for each experiment. All samples were dried under vacuum at 80°C for one night before measurements.

Gel permeation chromatography. To obtain information about molecular weight changes during manufacturing, number average molecular weights (Mn) and weight average molecular weights (Mw) were determined using an OmniSec GPC (Malvern Panalytical, Malvern U.K.) equipped with two columns branded PLGel mixed-B as well as a refractive index detector. Fragments were cut from the injected samples and solubilized into THF at a concentration of 1 mg.ml^{-1}. Solutions were agitated during 15 min at 40°C and filtered through a 0.02 µm PTFE membrane filter before test. The temperature was set at 30°C, the flow rate was 1 mL. min^{-1} and the injection volume was 20 µL. The calibration curve was established from five Polystyrene Shodex® narrow standards of respective molecular weights of 1 864 000, 194 500, 30 300, 7350 and 945 g.mol^{-1}. Data acquisition and processing were performed using the OmniSEC software.

Mechanical analyses. Quasi-static tensile tests were conducted using an Instron 5900 universal testing machine (Instron, Norwood (MA), USA), with a maximum load capacity of 100 kN. The tensile strength, failure strain and modulus of the fabricated composites were measured according to ISO 527-4 standard. The strain of the composite samples was measured using a non-contact method based Advanced Video Extensometer (AVE) setup attached to the Instron UTM. Load was applied by displacement control with a rate of 1 mm/min to provide quasi-static loading condition. The tensile modulus was determined as the slope of the initial linear portion of the stress-strain curves. A linear regression was performed on increasing blocks of measurement points and the modulus was determined when the maximum correlation was reached.

Results and discussion

Surface modification of fibers

Fourier Transform Infra-red Spectroscopy. FTIR spectra of untreated (FF), alkali-treated (AFF and ABF for flax and bamboo fibers, respectively) and silane (SFF and SBF) treated fibers are shown in Figure 1. The functional groups of the untreated fiber surface and their related FTIR spectra were analyzed and are listed in Table 1.

The band at 1730 cm^{-1} corresponding to C = O stretching vibration of carboxylic acid and ester groups of hemicellulose which are present in the untreated fibers, decreases sharply after alkaline treatment, indicating that the hemicellulose and lignin components were easily removed by NaOH treatment.[12,14] Also the weak band observes at 1052 cm^{-1} after silane treatment of flax, may be due to the asymmetric stretching of Si-O-Si bond in (3-aminopropyl) triethoxysilane resulting of condensation reaction of hydrolysed silane

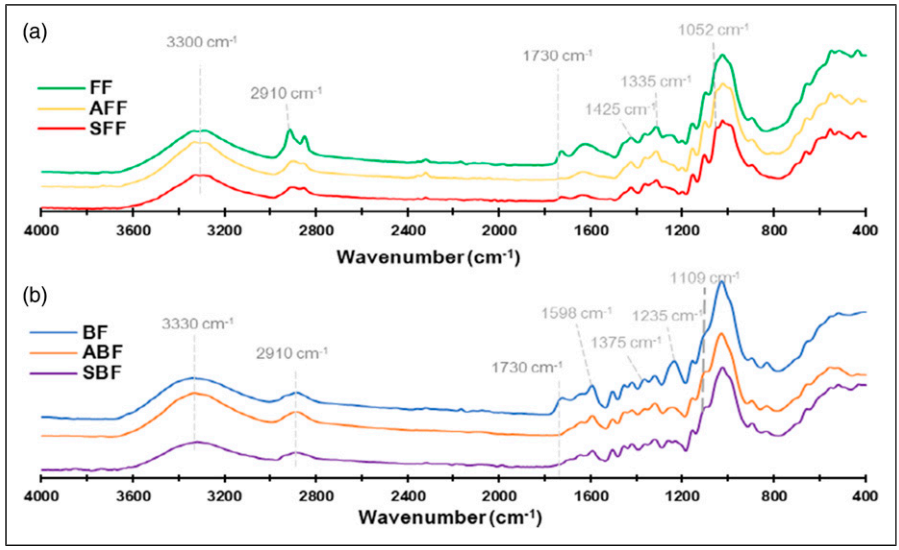

Figure 1. FTIR spectroscopy analysis of the surface-modified (a) Flax fibers (b) Bamboo fibers (normalisation band at 1018 cm^{-1}).

Table 1. FTIR data of untreated and silane treated fibers.

Wavenumber (CM^{-1})	Vibration	Source	Reference
3300	O–H linked shearing	Polysaccharides	18
2910	C–H stretching	Polysaccharides	15
1730	C=O stretching	Pectin, Hemicellulose, and Lignin	14
1598	C=C aromatic stretching	Lignin	19
1425	C-H shearing	Pectin, Lignin, Hemicelluloses	
1375	CH_2	Polysaccharides	
1335	C–O aliphatic ring	Cellulose	
1235	C–O aryl group	Lignin	
1109	Si-O-C	Silanization of bamboo	17
1075	C–O–C ether group of pyranoses	Cellulose, Hemicellulose	20
1052	Si-O-Si	Silanization of flax	21
1018	Si-O-Si	*(NORMALIZATION BAND)*	22
898	C–H glycosidic bonds	Polysaccharides	23

and hydroxyl groups of raw fiber cellulose.[14–16] Furthermore, a new band appears in the silane-treated fibers spectrum at 1109 cm^{-1} corresponding to the stretching vibration of Si–O–C.[15,17] These results demonstrate that chemical bonds have been formed after fibers being modified by the APS.

X-ray Photo-electron Spectroscopy. The surface chemistry of raw and silane-treated fibers was assessed from XPS spectroscopic analysis to confirm the functionalization of fibers. Figure 2 shows XPS survey spectra of electron intensity as a function of binding energy for untreated and silane-treated fibers. Each element produces a set of characteristic XPS peaks. These peaks correspond to the electron configuration within the atoms, e.g., 1s, 2s, 2p, 3s, etc. The number of detected electrons in each peak is directly related to the amount of element within the XPS sampling volume. By hence, the peaks around 533 eV and 285 eV correspond to the 1s oxygen and 1s carbon electron configuration O1s and C1s respectively, which are the features for all the lignocellulosic materials. Moreover, for both silane-treated bamboo and flax fibers, the absorption of silane-based APS on the surface of the fibers was identified from its characteristic emission peaks in the region between 99 and 104 eV for the Si2p, which can be better highlighted from a zoom from 90 to 110 eV.[24] Similarly, the presence of new nitrogen absorption peak at 399 eV is also identified for fibers treated from APTES containing the atom between 390 and 410 eV. The inset shows a quantification table (within Figure 2) indicating the atomic species, their atomic percentages and characteristic binding energies.

An increase in atomic % of oxygen and decrease of atomic % of nitrogen was observed compared to raw flax fibers (Figure 2(a) (1)). Whereas for silane-treated bamboo fibers

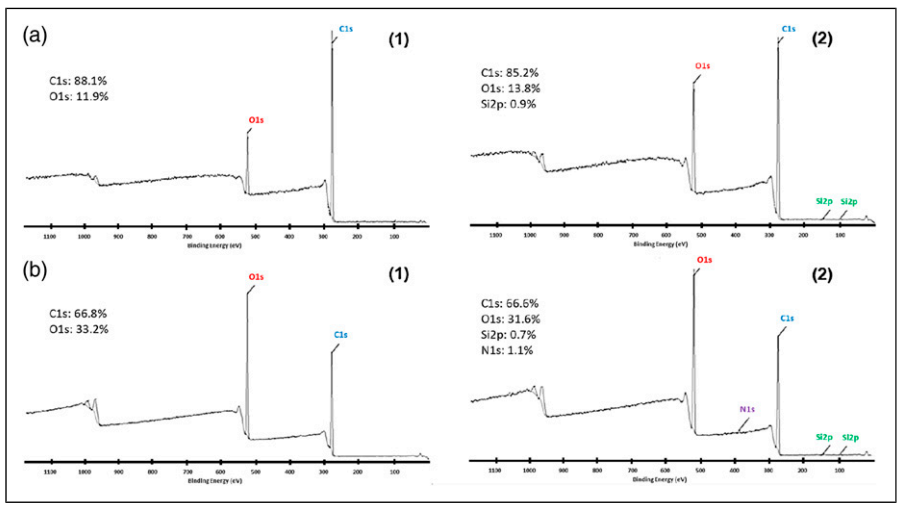

Figure 2. XPS survey spectra for Raw fibers: flax fibers A (1) and Bamboo fibers B (1), and Silane-treated fibers: flax fibers A (2) and Bamboo fibers B (2).

(Figure 2(b) (2)), characteristic peak of Si2p also appears but, contrary to flax, characteristic peak of nitrogen N1s appears at the same time as the decrease in atomic % of oxygen compared to raw bamboo fibers (Figure 2(b) (1)). Regarding the evolution of O and N for both treated fibers, it is clear that bamboo and flax fibers did not react in the same way during silanization. This could maybe due to the difference in their chemical composition.

Deconvolutions of the C1s, O1s and $Si2p_{1/2}$ and $Si2p_{3/2}$ peaks using a Gaussian function applied to the corresponding binding energies related to the peak positions are shown Figure 3 for flax fibers and Figure 4 for bamboo fibers.

The C1s peak deconvolution of raw fibers (Figure 3(a)(1) and Figure 4(a)(1) for FF and BF, respectively) and silane-treated fibers (Figure 3(b)(1) and Figure 4(b)(1) for FF and BF, respectively) show that scanned signal can be divided into three major components according to the chemical environment of the carbon atom: C-C around 284.8 eV; C-O bonds at 286.4 eV and C = O or O-C-O around 288 eV. On the one hand, for flax fiber, the deconvolution of peaks at specific bond energies after silane treatment shows the decrease in the atomic ratio of sp^3 C-C with an increase of both sp2 C = O (or O-C-O) bonds and strong rise of sp^3 C-O bonds. Yet, unlike the flax fiber, for bamboo fiber, the silanization induces a slight increase in the atomic ratio of sp^3 C-C bonds and a slight change in the atomic ratio of sp^3 and sp^2 C-O and C = O/O-C-O bonds. On the other hand, it can be noticed that C-O peaks moved from 286.3 to 286.4 eV and 286.4–286.5 eV and C = O peaks slightly shifted from 287.9 to 288.0 eV and 288.0–288.2 eV respectively for FF and FB, which might be caused by the shifts of C–OH to C–O–Si and C = O to C = O-O–Si.[25]

For O1s peak deconvolution of raw fibers (Figure 3(a)(2) and Figure 4(a)(2) for FF and BF, respectively) and silane-treated fibers (Figure 3(b)(2) and Figure 4(b)(2) for FF and BF, respectively), two peaks around 531.5 eV (O = C) and 532.9 eV (O-C) are noted. For the both fibers, the deconvolution of C-O and C = O peaks at specific bond energies after silane treatment indicates an increase of sp^2 C = O bonds and a decrease in the number of C-O bonds. Yet, the initiate ratio C-O/C = O is very different between both FF and FB fibers. As regards the FB, the majority of the initial functional groups are sp2 carbonyl bonds at more than 90% for FB while the proportion is lower for the same rate for FF. There is also a slight offset for the C-O groups of 0.1 eV for FB and no displacement for FF.

Finally, concerning the identification of the atomic environments of silicon in the form of two detected electronic configurations Si2p1 and Si2p3 (Figure 3(b)(3) and Figure 4(b)(3)), the deconvolution of the two fibers treated with APS silane shows several chemical changes in fiber surface. For the two fibrous reinforcements, it is noted, after treatment, the presence of silane bonds types Si-O-Si (101.5 eV) and Si-O (3) (102.6 eV). This means that there is a reactivity in the form of weak chemical interactions between the fiber and silane treatment without true covalent bonds or very weakly present on the surface of FF. In the case of flax fibers, we are more in the presence of links of physical interactions. However, for bamboo fiber, specifically, it is emphasized an additional bond by the Si-O (4) (28.1 at% of all possible chemical bonds of silicon) deconvolution located around 103.4 eV and characterizing the presence of a possible covalent interaction C-O-Si

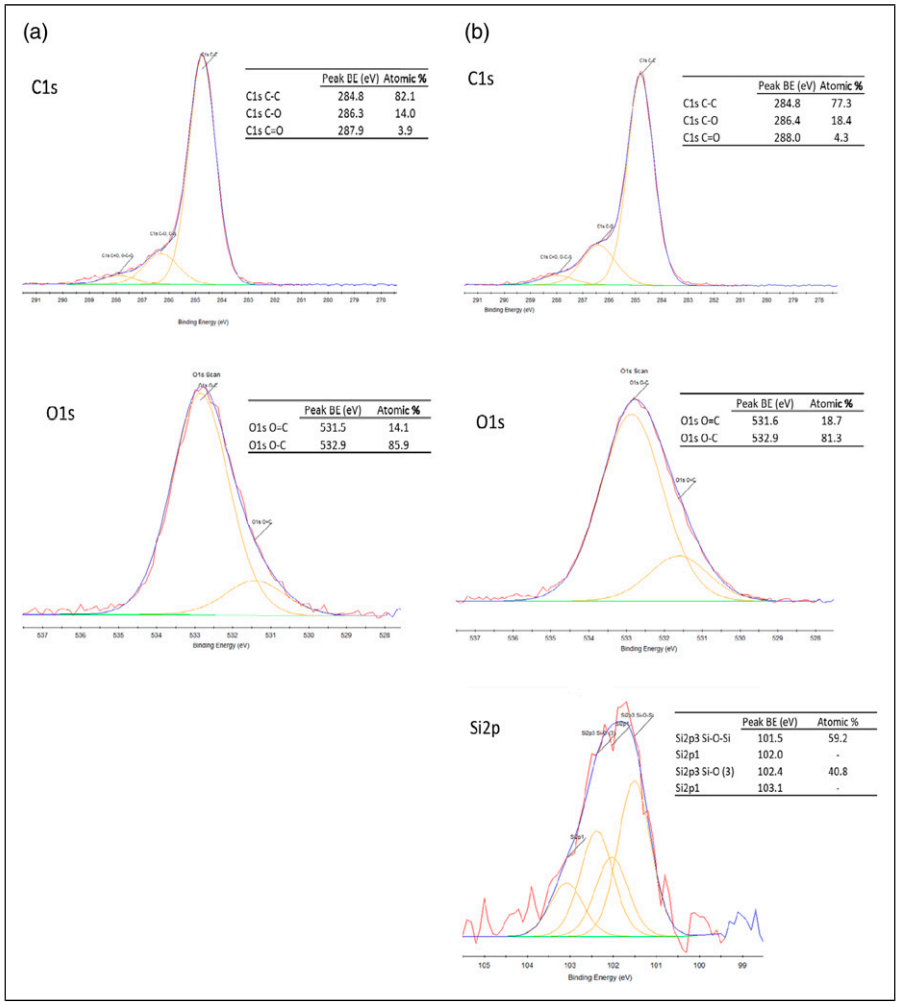

Figure 3. XPS deconvolution peaks of (a) raw flax: (1) C1s deconvolution, (2) O1s deconvolution and (b) silane-treated flax fibers: (1) C1s deconvolution, (2) O1s deconvolution and (3) Si2p deconvolution.

between the fibers and the APS treatment. There are thus several types of weak or strong interactions on the surface of the fibers, bamboo fibers being more chemically sensitive to the APS chemical system than flax fibers.

Moreover, the presence of a significant amount of nitrogen atom (1 at%) present on the surface of FB and not present on the surface of FF reinforces the idea of solid APS grafting.

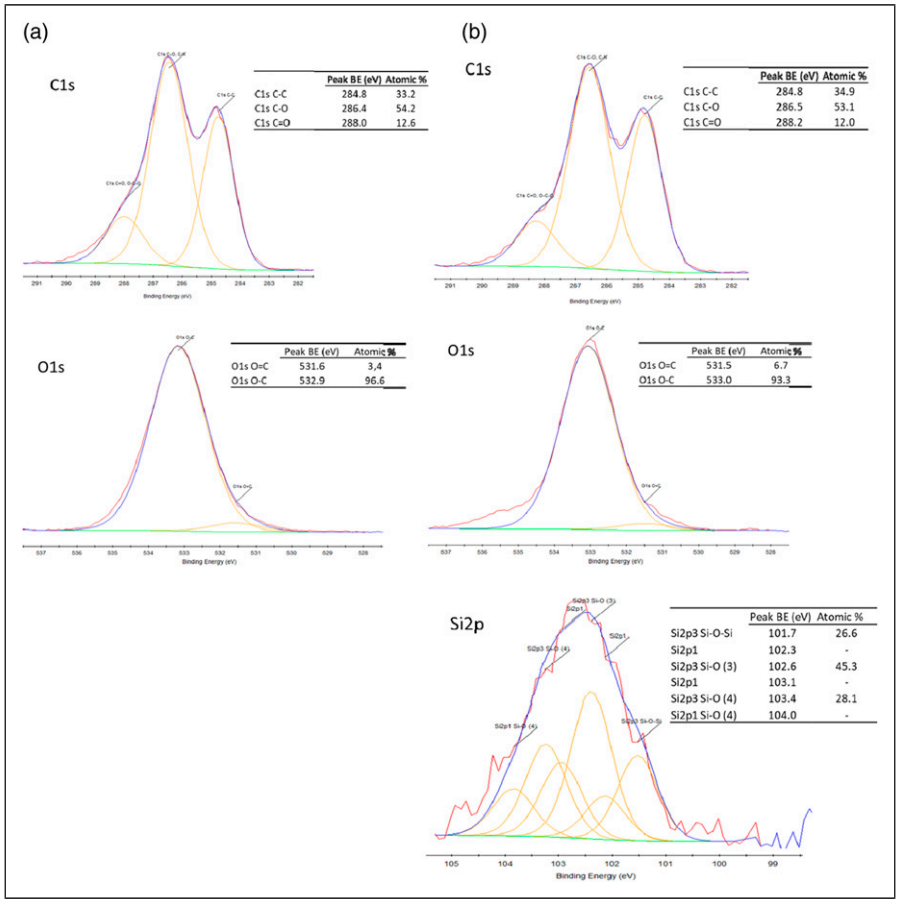

Figure 4. XPS deconvolution peaks of (a) Raw Bamboo fibers: (1) C1s deconvolution, (2) O1s deconvolution, (3) N1s deconvolution and (b) silane-treated Bamboo fibers: (1) C1s deconvolution, (2) O1s deconvolution, (3) N1s deconvolution and (4) Si2p deconvolution.

This result is consistent with the results obtained by Dorez et al[26] while grafting phosphonic acid bearing molecules onto lignin, cellulose and hemicellulose. In this article, it was shown that the phosphonated grafting agent reacted covalently with lignin but not with hemicellulose (xylan) and cellulose. It has been previously stressed that bamboo fibers have a higher content in lignin (around 21.7%) than flax fibers (around 2%).

Influence of silane and/or reactive agent treatments of fibers on the composite interface

SEM. SEM micrographs of the fractured surface of composites based on untreated, silane treated fibers and/or Joncryl treated composite are shown in Figure 5.

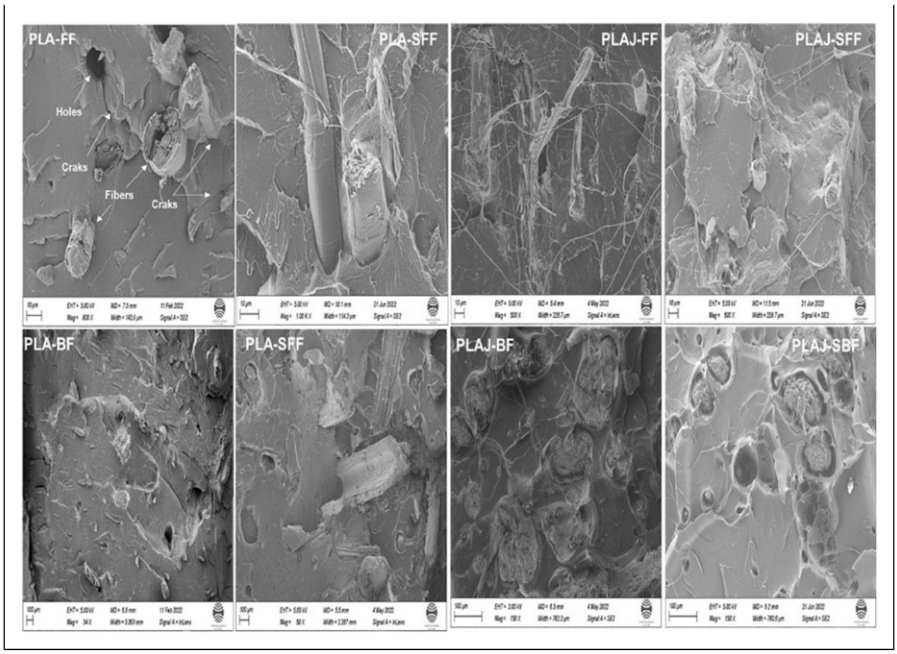

Figure 5. SEM micrographs of fractured cross-sections of PLA biocomposites.

PLA biocomposites (PLA-FF and PLA-BF) show cracks and voids in the matrix, resulting from the pull-out of the fibers and reflecting a poor interfacial adhesion between PLA matrix and fibers. PLA matrix exhibits a relatively smooth surface revealing a brittle fracture. Whereas for the composites based on silane-treated fibers, a strong fiber/matrix adhesion is observed with fibers difficult to tear off and a rough surface of the matrix cross section (probably due to a more difficult crack propagation). When Joncryl is added alone or in combination with the silane treatment, the fibers are still embedded in the matrix, and composite fracture appears around the fibers, with a stretching of the matrix. No voids or cracks on the matrix are observed. These observations for Joncryl containing composites reflect a significant modification in the mechanical properties of the matrix, changing the fracture behavior. Consequently, complementary investigations are needed to highlight improvement in the interfacial adhesion of PLA biocomposites due to the presence of the copolymer, which is able to react with the hydroxyl groups of cellulose.

Influence of silane treatment of fibers and/or reactive agent on thermal properties of composite

Thermogravimetric analyses. The thermal stability of biocomposites were investigated using TG analysis. Figure 6 shows the TG curve and derivative curves (DTG) of PLA and its biocomposites.

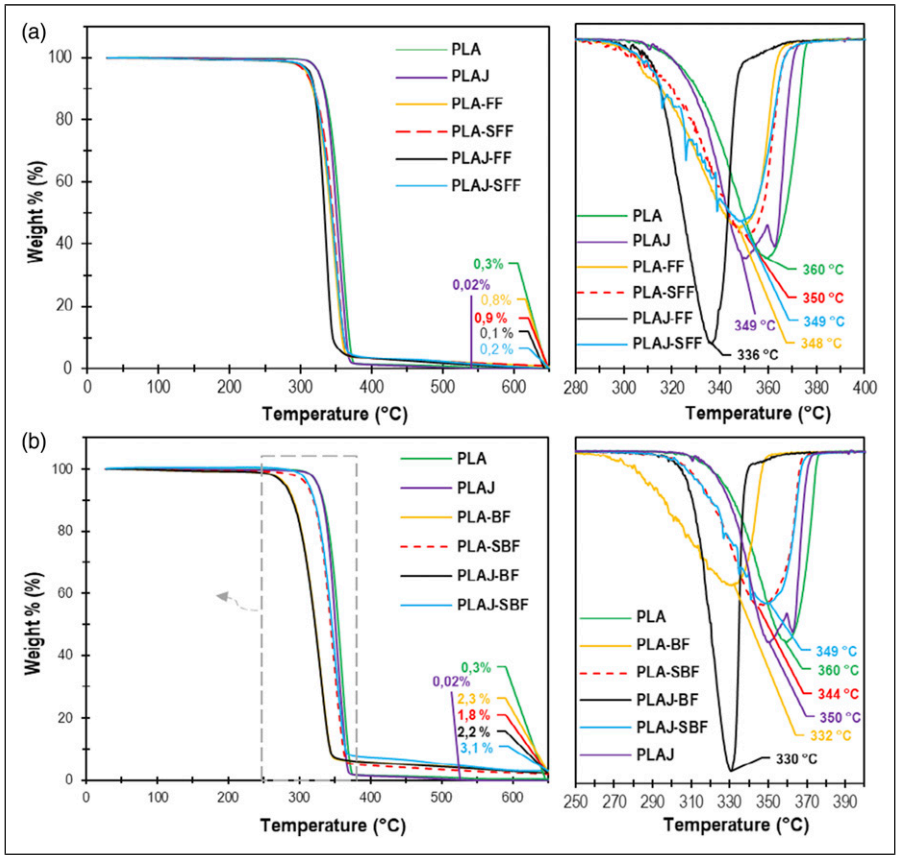

Figure 6. Thermal stability of PLA composite with raw and silane-treated fibers of (a) flax fibers and (b) bamboo fibers: TGA curves and DTG curves.

In TG curves, a first weight reduction should take place between 50°C and 250°C due to the loss of moisture and partial decomposition of hemicellulose present in natural fibers. But, it can be noted that composites exhibit no significant mass loss before 200°C. Indeed, the mixing temperature of composites is 185°C. Thus, the moisture in the material has almost completely disappeared. The main step of thermal degradation takes place between 260°C and 365°C and is due to the early stages of decomposition of PLA, and to the decomposition of hemicellulose, cellulose and lignin which overlap.[13,27] The last step of degradation is observed between 360°C and 460°C and is ascribed to the pyrolysis of residual lignin.[28]

DTG curves show a single-step degradation for PLA with a maximum degradation rate observed at 360°C (T_{max}), whereas the biocomposites PLA-FF and PLA-BF show a Tmax at 348°C and 332°C, respectively. Obviously, the incorporation of the fibers in the PLA

matrix considerably reduces its T_{max}, due to the respective temperatures of maximum degradation of around 160, 220, and 315°C for lignin, hemicellulose and cellulose in fibers.[23] However, with silane treatments of fibers, the thermal stability of biocomposites increases slightly with a T_{max} of 350°C for PLA-SFF and a T_{max} of 344°C for PLA-SBF in comparison with composites containing untreated fibers. The difference between flax and bamboo can be ascribed to the higher amount of silane grafted with bamboo than with flax, as shown with XPS. Moreover, all the compositions with bamboo lead to more residue than with flax due to a higher lignin content in bamboo fiber. Due to its aromatic structure, lignin leads to a charred residue.

The addition of Joncryl ADR 4468, a polymeric chain extender, decreases considerably the thermal stability of the corresponding composites. T_{max} of PLAJ-FF and PLAJ-BF are 336 and 330°C, respectively. However, with the addition of Joncryl combined with the silane coupling agent, the reality is quite different. The thermal stability increases considerably with a T_{max} of 349°C for both PLAJ-SFF and PLAJ-SBF. This relative loss of thermal stability could be explained by a specific reaction of Joncryl with the extractables eliminated by an alkaline treatment carried out before the reaction with silane. In this case, a part of Joncryl would not react with PLA or the fibre components and is released with extractive compounds at relatively low degradation temperature.

The DSC curves obtained from the second heat scan of different biocomposites are depicted in Figure 7 and the values of T_g, T_c, T_m, ΔH_c and ΔH_m obtained from DSC analysis are given in Table 2.

Compared to neat PLA (57°C), the values of Tg decrease after addition of fibers into the PLA matrix (53°C for both PLA-FF and PLA-BF). This behavior is in good agreement with previous studies,[29] indicating changes in the degree of plasticization, also increasing mobility and free volume of the matrix chains by loose packing of fibers within the matrix due to poor interaction between the untreated ones and the PLA matrix.[30] With chemical

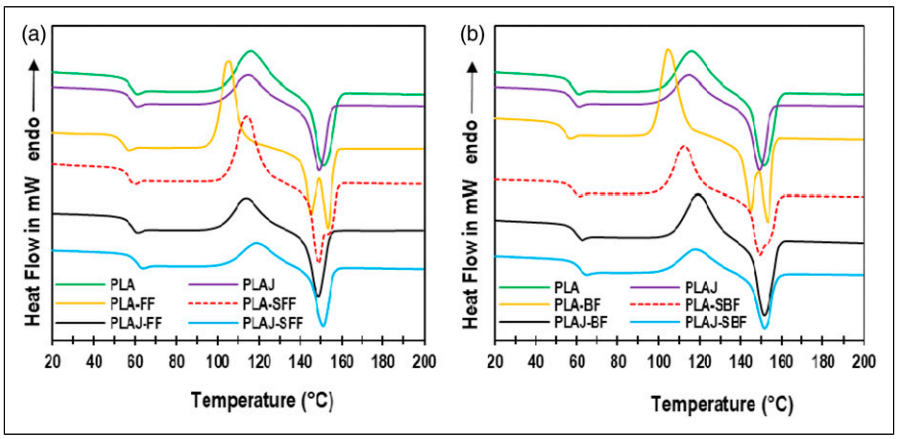

Figure 7. Summary of DSC characteristics, based on second heating scan thermograms of PLA and composites.

Table 2. DSC thermal properties of composites.

Materials	T_g (°C)	T_c (°C)	ΔH_c (J/G)	T_M (°C)	ΔH_M (J/G)	X_c (%)
PLA	57	112	14, 12	151	20, 59	22
PLAJ	57	114	6	149	15, 5	17
PLA-FF	53	105	24, 38	144-153	25, 1	30
PLA-SFF	56	114	22, 58	149	23, 34	29
PLAJ-FF	57	113	9, 16	149	16, 26	19
PLAJ-SFF	59	117	6, 16	151	14, 14	17
PLA-BF	53	105	26, 70	144-153	28, 30	34
PLA-SBF	57	112	17, 44	149	19, 27	23
PLAJ-BF	58	118	14, 34	151	19, 17	23
PLAJ-SBF	60	116	6, 17	152	13, 73	16

treatment of fibers, this interaction is enhanced due to a better affinity with the matrix, resulting in less mobility, and consequently an increase of the value of Tg for all silane-treated biocomposites (56 and 57°C for PLA-SFF and PLA-SBF, respectively) compared to the corresponding untreated fiber-based composite. Hence, a similar value as virgin PLA is recovered. The addition of Joncryl alone leads to a similar result (57°C and 58°C for PLAJ-FF and PLAJ-BF, respectively). The combination of the Joncryl with silane treatment entails a further increase of Tg (59 and 60°C for PLAJ-SFF and PLAJ-SBF, respectively).

The cold crystallization temperature of PLA is observed at Tc = 112°C, this temperature declined after the incorporation of fibers (Tc = 105°C for both composites PLA-FF and PLA-BF). This decline in the Tc can be attributed to shorter molecular chains and increased number of fibers ends within the PLA matrix which are expected to enhance the crystallization rate of the biocomposite, enabling it to crystallize at lower temperatures. The silane coupling agent provides effective interfacial interactions between PLA and fibers and restricts the movements of PLA chains. Therefore, the crystal growing rates of PLA-SFF (Tc = 114°C) and PLA-SBF (Tc = 112°C) composites could be slower than that of PLA-FF/PLA-BF.[31] The Tc is enhanced with the addition of Joncryl alone, which means that PLAJ-FF (Tc = 113°C) or PLAJ-BF (Tc = 116°C) composites need higher temperature to regain chain segments movement ability in comparison with that of PLA-FF/PLA-BF composites. In addition, the specific structure of PLAJ in comparison with PLA (comb-type polymer structure) is prone to reduce its ability to crystallize.[9,10]

Therefore, the restricted chain movement ability of PLAJ-FF and PLAJ-BF composites is demonstrated.[32] Moreover, the addition of Joncryl combined with the silane coupling agents provides even more efficient interfacial interactions between the PLA and the fibers and further limits the movements of the PLA chains. Therefore, it can be suggested that the crystal growth rates of PLAJ-SFF (Tc = 117°C) composites and PLAJ-SBF (Tc = 118°C) composites are even slower than those of PLA.

The melting temperature of PLA is observed at 151°C whereas the corresponding biocomposites PLA-FF and PLA-BF show double peaks at 144 and 153°C. The first

melting peak can be attributed to the melting of imperfect crystallites, formed during cold crystallization upon heating, and second one to the melting of new crystallites formed through the melt-recrystallization process.[33]

Rheology

The rheological investigations were carried out to evaluate the thermal stability of PLA and its biocomposites. From Figure 8, it is shown that the complex viscosity of PLA decreases slightly from 2990 Pa.s to 2904 Pa.s at 185°C in 40°min, i.e. 3%. The decrease in viscosity observed for pure vacuum-dried PLA is ascribed to strictly thermal degradation mechanisms that take place, corresponding to a loss in molecular weight. In addition to this phenomenon, it has been shown that the incorporation of fibers into PLA matrix induces its degradation by hydrolysis processes.[34] Fibers promote hydrolytic degradation of the PLA matrix because of the water bound to the hydroxyl groups of the main fiber constituents, namely cellulose, hemicelluloses, pectins, and lignins.[13] The complex viscosity of the corresponding composites drops and decreases by 39% for PLA-FF (from 2160 to 1312 Pa.s) and by 57% for PLA-BF (from 2487 to 1062 Pa.s).

Once the fibers have been treated by alkalization and silanization, this treatment reduces the bound water of the fibers inducing hydrophobization. These pretreatments modify the degradation kinetics of PLA composites since both the slope and magnitude of the complex viscosity decreases are significantly reduced for the corresponding composites, i.e. 22% and 26% for PLA-SFF and PLA-SBF, respectively.

Strong differences in the rheological response of all compositions containing Joncryl are observed. Moreover, for all these compositions, the complex viscosity is considerably increased compared to the compositions without Joncryl.[35] It is particularly the case for biocomposites with silane treated fibers. This can be ascribed to the formation of branched structures in addition to linear ones. From Najafi et al.,[9] carboxyl end groups of PLA chains react with the side chains of Joncryl copolymer bearing epoxy groups, leading to a comb-like structure (Figure 9).

However, the viscosity tends to level off or even decrease during time sweep test, for untreated fibers despite the use of Joncryl. This can also be attributed to the detrimental influence of untreated fibers on PLA hydrolysis.

GPC

To fully understand the chain extension/branching and silane treatment balance occurring during reactive processing the measurements of average molecular weight have been carried out. The weight (Mw) and number (Mn) average molecular weights, and polydispersity ($\frac{M_w}{M_n}$) of PLA composite are given in Table 3 and presented in Figure 10.

The incorporation of fibers in PLA matrix (Mn = 119 677g.mol^{-1} and Mw = 219 288 g.mol^{-1}) leads to hydrolyzation processes, which induce chain scission, molecular weight reduction (Mn = 78061 g.mol^{-1} and Mw = 135649 g.mol^{-1} for PLA-FF; Mn = 68 488 g.mol^{-1} and Mw = 97 460 g.mol^{-1} for PLA-BF) and possible formation of

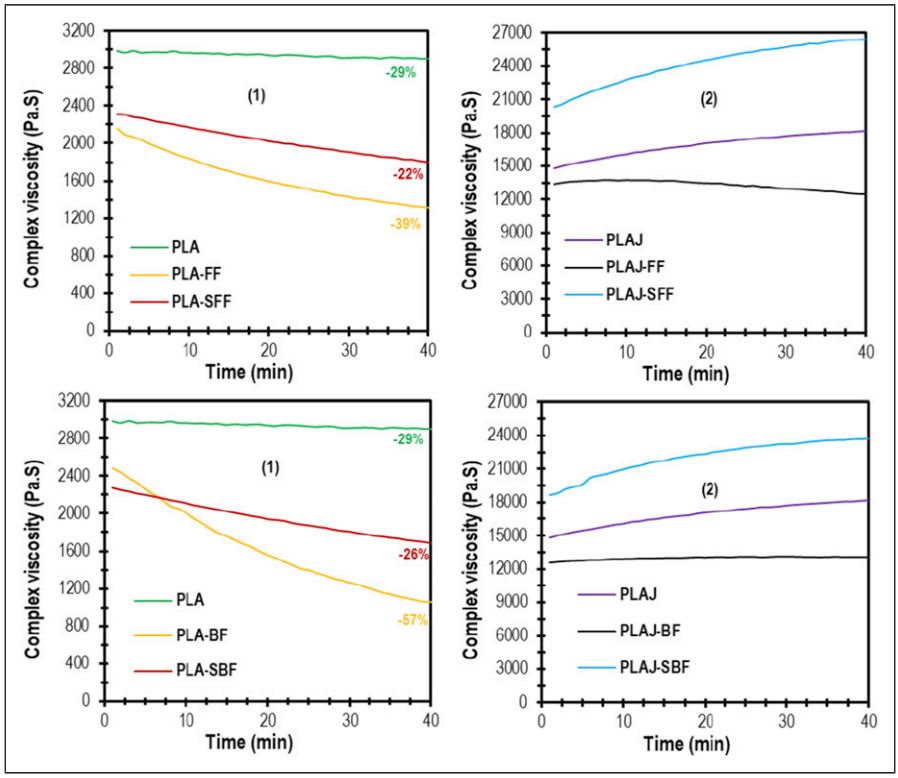

Figure 8. Rheological behaviors of PLA composites.

new functional groups (-COOH, HOC-COOH). Added alone or with silane coupling agent in the formulation, the Joncryl chain extenders can react with the PLA chain ends forming a branched network, thus increasing the Mn (183 601, 189 504, 155 612 and 167 408 $g.mol^{-1}$ for PLAJ-FF, PLAJ-SFF, PLAJ-BF and PLAJ-SBF, respectively) and Mw (504 247, 470 424, 500 903 and 494 088 $g.mol^{-1}$ for PLAJ-FF, PLAJ-SFF, PLAJ-BF and PLAJ-SB, respectively). The carboxyl terminal groups of the PLA react with the Joncryl epoxy groups, which lengthens the polymer chain.[23] As expected, the surface treatment of fibers with APS leads to an increase in average molecular weight of the corresponding composites (Mn = 83973 $g.mol^{-1}$ and Mw = 144 466 $g.mol^{-1}$ for PLA-SFF; Mn = 84 731 $g.mol^{-1}$ and Mw = 160 515 $g.mol^{-1}$ for PLA-SBF) in comparison with the composites reinforced with the unmodified fibers. Table 3 also reveals that the addition of Joncryl (whatever the composition) leads to an increase in the polydispersity index. This shows that the crosslinking is not homogeneous in the composite probably due to the low residence time in twin screw extrusion. All these results are consistent with the rheological properties shown in Figure 8.

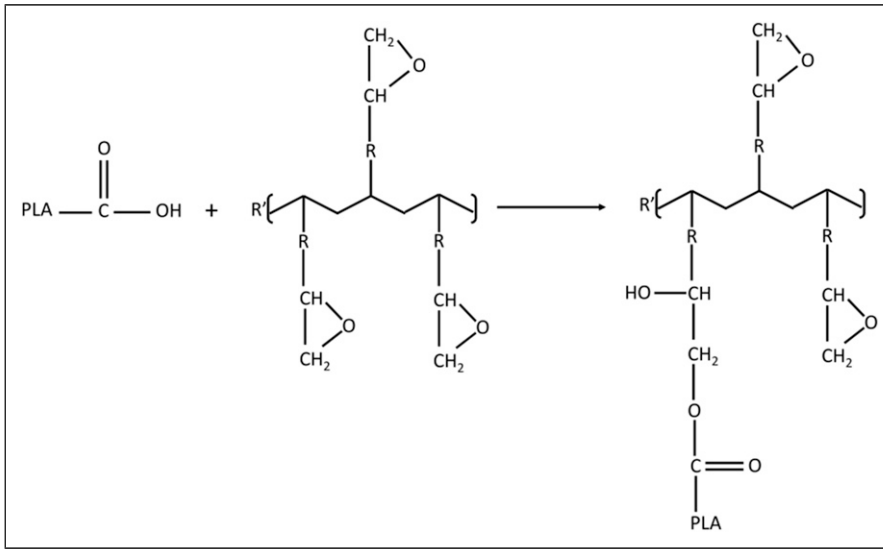

Figure 9. Reaction of Joncryl copolymer according to Najafi et al.[9]

Table 3. Number average molecular weight (Mn), weight average molecular weight (Mw), and polydispersity index of PLA composite.

Materials	MN (G/MOL)	MW (G/MOL)	PDI
PLA	119 677	219 288	1.83
PLAJ	237 137	586 753	2.47
PLA-FF	78 061	135 649	1.74
PLA-SFF	83 973	144 466	1.72
PLAJ-FF	183 601	504 247	2.75
PLAJ-SFF	189 504	470 424	2.48
PLA-BF	68 488	97 460	1.42
PLA-SBF	84 731	160 515	1.89
PLAJ-BF	155 612	500 903	3.22
PLAJ-SBF	167 408	494 088	2.95

Influence of silane treatment of fibers and/or reactive agent on mechanical properties

Tensile tests. The mechanical properties of PLA and different composites are shown in Figure 11. Compared to PLA (E = 3.2 GPa), the addition of 10% flax and bamboo fibers in matrix PLA increases the tensile modulus, leading to PLA-FF (E = 3.6 GPa) and PLA-BF (E = 3.8 GPa) composites by about 10% and 16%, respectively. This was attributed to the higher modulus of fibers in comparison to that of the matrix allowing the loading capacity of the composites to be greatly enhanced.[32] Nevertheless, the tensile strength decreases by

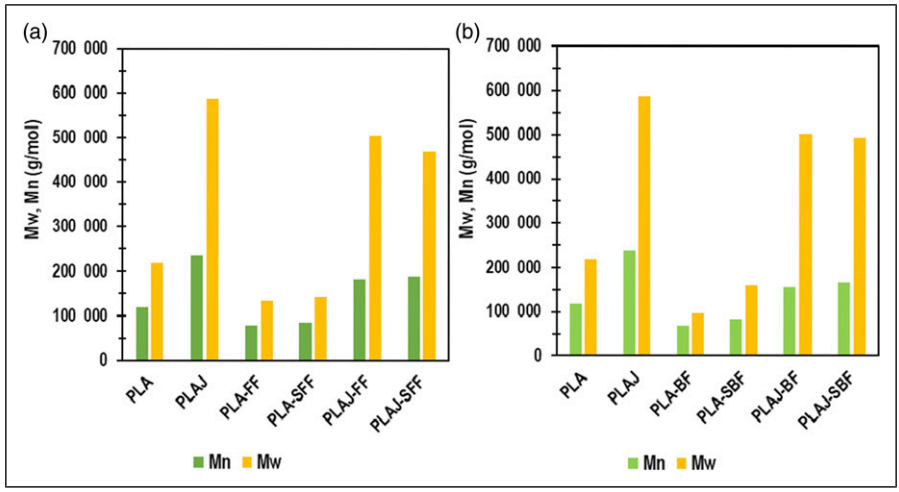

Figure 10. Molecular weights measurements of PLA composites ((a) Flax-based and (b) Bamboo-based fibers).

12% for both corresponding composites PLA-FF and PLA-BF (from about 57 MPa to 50 MPa), which may be due to a poor interfacial adhesion between natural fiber and matrix.

The silane treatment of the fibers results in a slight improvement of the tensile modulus, possibly due to a reduction of the influence of the fibers on the hydrolysis of PLA. The increase is the most significant for flax fibers. A positive influence of the silane is also noted on the tensile strength of the corresponding composites but the increase is observed mainly for PLA-SFF (from about 50 MPa to 54 MPa), whereas only a slight evolution is noted for PLA-SBF (from about 50 MPa to 51 MPa).

Joncryl added alone or in combination with silane coupling agent leads to further increase for both tensile modulus and tensile strength.

The use of Joncryl alone is beneficial on both tensile modulus and strength for both composites. An increase of 10% and 8% for tensile modulus of PLAJ-FF and PLAJ-BF, respectively is achieved in comparison to the PLA-FF and PLA-BF reference composites, whereas improvements of 8% and 4% for tensile strength are noticed respectively in comparison with the reference composites reinforced with untreated fibers.

It can be noticed that for PLAJ-FF composite, the tensile strength is maintained at about 58 MPa as for PLAJ, showing a very good load transfer at the fiber/matrix interface. For PLAJ-BF composite, only a decrease of about 4 MPa in comparison with PLAJ is observed. Consequently, since the use of Joncryl allows to reduce significantly the loss of tensile strength of PLA in presence of fibers, it can be considered that it will play the role of a coupling agent. The better efficacy of Joncryl towards flax can be explained by its larger interfacial area available in comparison with bamboo due to the higher diameter of bamboo fibers in the composites (Figure 12).

The combination of silane treatment and Joncryl addition is particularly advantageous since an increase of the tensile modulus of 17 and 11% is achieved for PLAJ-SFF and PLAJ-SBF composites, respectively in comparison with the reference composites. The same comparisons for the tensile strength entailed improvements of 20% and 16%,

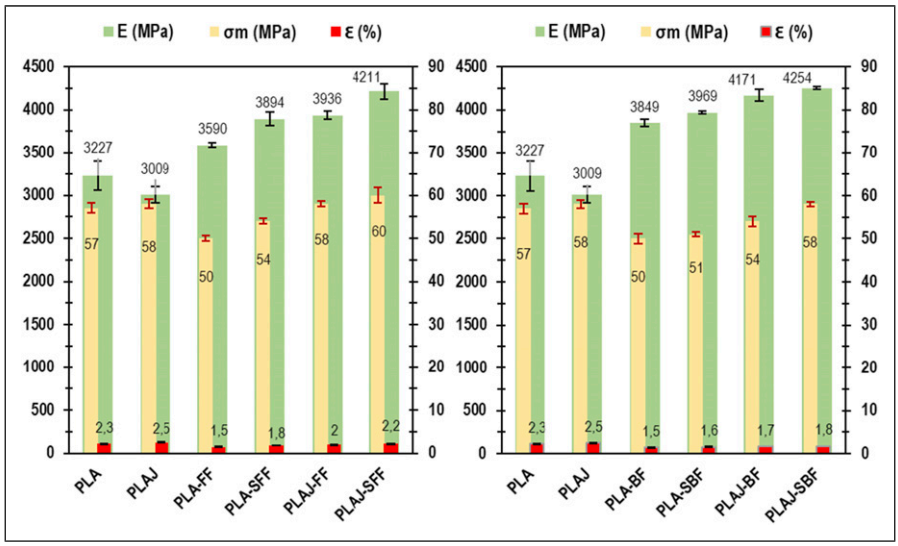

Figure 11. Mechanical tensile testing of (a) flax composites (b) bamboo composites. Young modulus E, tensile strength σ and strain at break ε are reported.

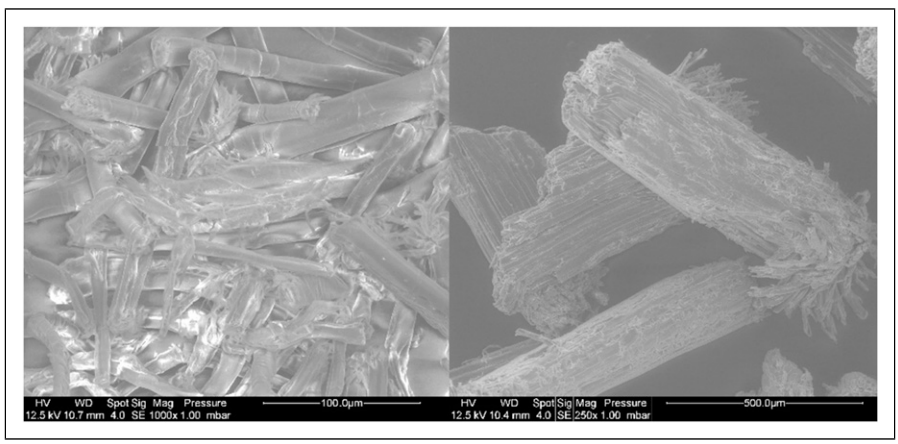

Figure 12. Aspect of flax (left) and bamboo fibers (right) from PLAJ-SFF and PLAJ-SBF composites after Soxhlet extraction of PLA, respectively.

respectively. Moreover, it can be noticed that for both composites with silane treatment and Joncryl addition, tensile strength obtained are higher than this of pristine PLA.

In addition, strain at break is not significantly modified for PLAJ-FF and PLAJ-BF composites in comparison with pure PLA despite strain of PLA (2.3%) is reduced with the introduction of fibers (1.5% for PLA-FF and PLA-BF). After silane treatment, Joncryl added alone and in combination with silane coupling agent. Strain increased to 1.8%, 2% and 2.2% for PLA-SFF, PLAJ-FF and PLAJ-SFF respectively; and also increased to 1.6%, 1.7% and 1.8% for PLA-SBF, PLAJ-BF and PLAJ-SBF. Clearly, different treatments on PLA composites increase the strain properties which remain anyway very low, considering the mechanical behavior of pristine PLA.

Conclusion

This study aimed to assess the influence of silane treatment and/or a reactive agent as Joncryl on the properties of PLA biocomposite. The effect of silane treatments on the interfacial properties of fibers (flax and bamboo), as well as the addition of chain extender alone or in combination, on the resulting thermal and mechanical properties of reinforced poly (lactic acid) (PLA) biocomposites have been studied.

Both FTIR and XPS spectroscopies confirmed that the APS silane coupling agent was covalently grafted on bamboo fibers probably thanks to their high amounts of lignin. Whereas only weak interactions were created in the case of flax fibers. It is probable that in the late case, silane was forming a coating around the flax fiber, but this would need more investigation to be proven.

The untreated flax and bamboo fibers weaken the PLA thermal degradation (as shown by TGA and rheology), possibly ascribed to the hydrolysis phenomenon. This thermal degradation leads to an increase of the macromolecular mobility and decrease in glass transition temperature (shown by DSC). Even if the accelerated thermal degradation of PLA is still present when fibers are treated with silane, the fiber/matrix interactions were improved (seen by cryo-fractured profile in SEM), resulting in increasing values of Tg and lower losses of complex viscosity during the time sweep rheological test. This was even more evident when Joncryl was added to the treated fibers.

The addition of Joncryl created crosslinking in the PLA network, due to the reaction between epoxy groups of Joncryl and PLA chain ends. This had the consequence to increase the molecular weight of the composites (seen by rheology and GPC) but also to increase the polydispersity of the PLA chains. Moreover, it can be also suggested that Joncryl could react with some extractible present in the fibers. Both kinds of reactions can account for the decrease in thermal stability of PLAJ-BF and PLAJ-FF composites. The combination of silane and Joncryl in the composites dramatically improve the complex viscosity and its evolution during time as if the crosslinking reaction was not complete during the extrusion (for which resident time is low) and was prolonged under the rheometer. The use of the copolymer allows the benefit of silane on mechanical properties to be enhanced as additional coupling agent.

PLAJ-SFF and PLAJ-SBF are then promising composites with interesting improved tensile elastic modulus and stabilized tensile strength (compared to neat PLA and

composites with untreated fibers). Complementary work on durability and recyclability of these biocomposites has been carried out and will be submitted shortly.

Acknowledgements

This study is part of the RecComBioS project entitled "Recyclability of Biosourced Composites", supported and funded by the Carnot M.I.N.E.S Institute.

Declaration of conflicting interests

The author(s) declared no potential conflicts of interest with respect to the research, authorship, and/or publication of this article.

Funding

The author(s) disclosed receipt of the following financial support for the research, authorship, and/or publication of this article: This study is supported by Institut Carnot MINES.

References

1. Baley C, Bourmaud A and Davies P. Eighty years of composites reinforced by flax fibres: a historical review. *Comp. Part A: Appl. Sci. Manuf* 2021; 144: 106333.
2. Vinod A, Sanjay MR and Suchart S. Recently explored natural cellulosic plant fibers 2018–2022: a potential raw material resource for lightweight composites. *Ind Crops Prod* 2023; 192: 116099.
3. Afifah Binti Taib NA, Rezaur Rahman M, Hudu D, et al. A review on poly lactic acid (PLA) as a biodegradable polymer. *Polymer Bulletin* 2023; 80: 1179–1213.
4. Farah S, Anderson DG and Langer R. Physical and mechanical properties of PLA, and their functions in widespread applications — a comprehensive review. *Adv Drug Deliv Rev* 2016; 107: 367–392.
5. Rajeshkumar G, Arvindh Seshadri S, Devnani GL, et al. Environment friendly, renewable and sustainable poly lactic acid (PLA) based natural fiber reinforced composites – a comprehensive review. *J Clean Prod* 2021; 310: 127483.
6. Zhang K, Chen Z, Boukhir M, et al. Bioinspired polydopamine deposition and silane grafting modification of bamboo fiber for improved interface compatibility of poly (lactic acid) composites. *Int J Biol Macromol* 2022; 201: 121.
7. Hasan A, Rabbi MS and Maruf Billah M. Making the lignocellulosic fibers chemically compatible for composite: a comprehensive review. *Clean. Mat* 2022; 4: 100078.
8. Hao MY, Wu HW, Qiu F, et al. Interface bond improvement of sisal fibre reinforced polylactide composites with added epoxy oligomer. *Materials* 2018; 11(3): 22.
9. Najafi N, Heuzey MC and Carreau PJ. Polylactide (PLA)-clay nanocomposites prepared by melt compounding in the presence of a chain extender. *Compos Sci Technol* 2012; 72(5): 608–615.
10. Rasselet D, Caro-Bretelle AS, Taguet A, et al. Reactive compatibilization of PLA/PA11 blends and their application in additive manufacturing. *Materials* 2019; 12(3): 18.

11. Cisneros-Lopez EO, Pal AK, Rodriguez AU, et al. Recycled poly(lactic acid)–based 3D printed sustainable biocomposites: a comparative study with injection molding. *Mat. Today Sustain* 2020; 7-8: 100027.
12. Backes EH, De N, Pires L, et al. Analysis of the degradation during melt processing of PLA/biosilicate composites. *J. Compos. Sci* 2019; 3: 52.
13. Dorez G, Ferry L, Sonnier R, et al. Effect of cellulose, hemicellulose and lignin contents on pyrolysis and combustion of natural fibers. *J Anal Appl Pyrol* 2014; 107: 323–331.
14. Gierlinger N, Goswami L, Schmidt M, et al. In situ FT-IR microscopic study on enzymatic treatment of poplar wood cross-sections. *Biomacromolecules* 2008; 9: 2194–2201.
15. Sabarinathan P, Rajkumar K, Annamalai VE, et al. Characterization on chemical and mechanical properties of silane treated fish tail palm fibres. *Int J Biol Macromol* 2020; 163: 2457–2464.
16. Hong CK, Hwang I, Kim N, et al. Mechanical properties of silanized jute-polypropylene composites. *J Ind Eng Chem* 2008; 14: 71–76.
17. Lu TJ, Jiang M, Jiang ZG, et al. Effect of surface modification of bamboo cellulose fibers on mechanical properties of cellulose/epoxy composites. *Compos. Part B-Eng* 2013; 51: 28–34.
18. Pandey KK. A study of chemical structure of soft and hardwood and wood polymers by FTIR spectroscopy. *J Appl Polym Sci* 1999; 71: 1969–1975.
19. Gordobil O, Egues I and Labidi J. Modification of Eucalyptus and Spruce organosolv lignins with fatty acids to use as filler in PLA. *React Funct Polym* 2016; 104: 45–52.
20. Spinace MAS, Lambert CS, Fermoselli KKG, et al. Characterization of lignocellulosic curaua fibres. *Carbohydrate Polymers* 2009; 77: 47–53.
21. Pena-Alonso R, Rubio F, Rubio J, et al. Study of the hydrolysis and condensation of gamma-aminopropyltriethoxysilane by FT-IR spectroscopy. *J Mater Sci* 2007; 42: 595–603.
22. Lee J, Kim J, Kim H, et al. Effect of thermal treatment on the chemical resistance of Polydimethylsiloxane for microfluidic devices. *J Micromech Microeng* 2013; 23: 035007.
23. Sinha E. Effect of cold plasma treatment on macromolecular structure, thermal and mechanical behavior of jute fiber. *J Ind Text* 2009; 38: 317–339.
24. Fang L, Chang L, Guo WJ, et al. Influence of silane surface modification of veneer on interfacial adhesion of wood-plastic plywood. *Appl Surf Sci* 2014; 288: 682–689.
25. Yang H, Hou D, Zheng D, et al. Mechanical properties and mechanisms of alkali-activated slag paste reinforced by graphene oxide-SiO2 composite. *J Clean Prod* 2022; 378: 134502.
26. Dorez G, Otazaghine B, Taguet A, et al. Use of Py-GC/MS and PCFC to characterize the surface modification of flax fibres. *J Anal Appl Pyrol* 2014; 105: 122–130.
27. Yang HP, Yan R, Chen HP, et al. Characteristics of hemicellulose, cellulose and lignin pyrolysis. *Fuel* 2007; 86: 1781–1788.
28. Brebu M and Vasile C. Thermal degradation of lignin- a review. *Cellul Chem Technol* 2010; 44: 353–363.
29. Qiu ZB and Yang WT. Crystallization kinetics and morphology of poly(butylene succinate)/poly(vinyl phenol) blend. *Polymer* 2006; 47: 6429–6437.
30. Jandas PJ, Mohanty S and Nayak SK. Thermal properties and cold crystallization kinetics of surface-treated banana fiber (BF)-reinforced poly(lactic acid) (PLA) nanocomposites. *J Therm Anal Calorim* 2013; 114: 1265–1278.

31. Hong HQ, Xiao RJ, Guo QN, et al. Quantitively characterizing the chemical composition of tailored bagasse fiber and its effect on the thermal and mechanical properties of polylactic acid-based composites. *Polymers* 2019; 11: 20.
32. Xiong Z, Yang Y, Feng JX, et al. Preparation and characterization of poly(lactic acid)/starch composites toughened with epoxidized soybean oil. *Carbohydrate Polymers* 2013; 92: 810–816.
33. Georgiopoulos P and Kontou E. The effect of wood-fiber type on the thermomechanical performance of a biodegradable polymer matrix. *J Appl Polym Sci* 2015; 132: 10.
34. Mazzanti V, de Luna MS, Pariante R, et al. Natural fiber-induced degradation in PLA-hemp biocomposites in the molten state. *Compos. Part A-Appl. Sci. Manuf* 2020; 137: 7.
35. Standau T, Nofar M, Dorr D, et al. A review on multifunctional epoxy-based Joncryl® ADR chain extended thermoplastics. *Polym Rev* 2022; 62: 296–350.